Excitonic superradiance to exciton-polariton crossover and the pole approximations

Gunnar Björk, Stanley Pau, Joseph M. Jacobson, Hui Cao, and Yoshihisa Yamamoto
ERATO Quantum Fluctuation Project, Edward L. Ginzton Laboratory, Stanford University, Stanford, California 94305
(Received 11 May 1995; revised manuscript received 8 August 1995)

We examine the relationship between atomic and excitonic superradiance in thin and thick slab geometries. We demonstrate that superradiance can be treated by a unified formalism for atoms, Frenkel excitons, and Wannier excitons. It is well known that in sufficiently thick slabs, the normal modes of the system are polaritons, a superposition of the slab exciton, and photon modes. We specifically examine the crossover from superradiance to polariton modes and derive both the crossover slab length and the maximum superradiative decay rate. We show that the exciton and polariton pole approximations, which give simple expressions for superradiance and polariton mode decay rates, give excellent agreement with the exact expressions for the pertinent thicknesses for which the approximations are valid.

I. INTRODUCTION

Atomic superradiant decay was proposed by Dicke[1] as a way for mutually phase-coherent atoms to decay at a substantially faster rate than the single atom decay rate. If N coherently evolving atoms are located in a volume much smaller than a wavelength cubed, the radiative decay rate can be increased by a factor N provided their dipole moment evolves in phase. If the atom's respective dipole moments are mutually out of phase, Dicke also showed that the radiation may be totally quenched. Such an atomic state is called a dark state or a radiation trapped state. Several groups[2–6] subsequently calculated the superradiant decay rate for systems where the atoms have a spatial distribution larger than a wavelength cubed. They found that in general the superradiant decay rate is smaller than the factor N due to the fact that any two atoms separated by more than the distance of an inverse wave vector cannot emit radiation in phase (or cooperate) in all spatial directions. However, in their formalisms no upper limit for the superradiant decay rate enters explicitly. About the same time Arecchi and Courtens[7] warned that, used without caution, superradiance calculations would predict impossibly large decay rates, e.g., decay rates larger than the optical transition frequency. Arecchi postulated a maximum cooperativity distance, and with that most of the workers in the field seem to have been content. In geometries thinner than the longitudinal cooperativity distance, this problem does not arise. Quite early Lee and Lee[5] calculated superradiant decay rates in thin molecular films and Hanamura[8] calculated the decay rate for semiconductor excitons in microspheres and in planar geometries. Recently Knoester[9,10] pointed out that in superradiance calculations the radiation reaction (absorption of emitted radiation) is usually ignored. This is the so called exciton pole approximation. In the exciton pole approximation, radiative shifts are also often ignored, although they do not have to be. In reality, superradiance is accompanied by radiative shifts, as pointed out in (Ref. 11). However, Knoester's main objection to the exciton pole approximation coincides with that of Arecchi and Courtens; the thin-film results cannot be extrapolated to thick slabs with impunity. Knoester derived the proper (no pole approximation) equation of motion for the normal modes of a crystal slab. He demonstrated that the fundamental, $\mathbf{k} = 0$ mode shows superradiant behavior and that it has a maximum radiative decay rate when the crystal slab thickness is half a wavelength. He also predicted that higher-order modes had larger decay rates, but no result was presented. However, he showed that in sufficiently thick slabs the normal modes of the system are the radiatively stable polariton modes.[12]

In this paper we demonstrate that Arecchi and Courtens' postulate arises naturally in Knoester's pole approximation-free theory. Recently several authors[13–17] have pointed out that exciton superradiance can be enhanced by enclosing the superradiant slab in a planar microcavity. In (Refs. 13, 14, 16, and 17) the exciton pole approximation was not employed, and the respective treatments show that the excitonic superradiance gives way to microcavity excitonic polaritons as soon as the microcavity mirror reflectivity becomes sufficiently high, provided that the excitons are not localized, e.g., by impurities. In Refs. 16 and 17 the mirror reflectivity needed for the superradiance to exciton-polariton crossover to occur was explicitly calculated. In Ref. 15, on the other hand, a generalized treatment applicable to atoms, Frenkel excitons, and Wannier excitons was used, and so was the exciton pole approximation. In Ref. 15, it was predicted that the crossover would occur when the microcavity-enhanced superradiant decay rate exceeded the cavity decay rate. It was demonstrated that the maximum microcavity-enhanced superradiant decay rate was roughly equal to the Rabi flopping frequency. This was confirmed by Savona *et al.*[16] From the treatment in Ref. 15, it is clear that all superradiant atomic and excitonic processes, microcavity-enhanced or not, essentially are a manifestation of the same physics, namely, the formation of macroscopic (larger than a wavelength) dipole moments. The reason atomic and Wannier exciton superradiance previously have been treated as separate entities seems to be that in the former the atomic wave functions are highly localized, whereas in the case

of Wannier excitons the exciton wave functions are highly delocalized. However, if the atomic density is sufficiently high (the number of atoms per square wavelength in a thin film $\gg 1$), the collective wave function of the atoms is also delocalized, and the constituent atoms' respective wave functions cannot be resolved by an electromagnetic wave. Therefore, the two systems are equivalent in most respects.

In this paper we will concentrate on the weak excitation regime. For an excitonic system this is equivalent to keeping the exciton density much below the Mott density. For an atomic system it is equivalent to keeping the atom inversion very low. In the Bloch sphere picture, the Bloch vector must be kept close to the south pole (ground state). Hence every atom initially is assumed to be in a superposition of the ground and excited states, with the ground-state probability being dominant. In both the exciton and the two-level atom cases, the weak excitation will allow us to neglect the Coulomb-Coulomb interaction and exchange interaction. Effectively the system, even a collection of two-level atoms, can be treated as a single bosonic mode, and none of the nonlinear effects present in strongly excited two-level atomic systems[18–20] will be seen. It is worth pointing out that the superradiant decay rate for such a system is independent of the excitation level.

Rehler and Eberly early predicted that the maximum superradiant decay rate would be obtained when the photon-mode wave vector matched the atomic-state wave vector. In spite of this, most calculations of bare superradiant slabs have been focused on the slab fundamental $k = 0$ mode. The reason seems to be that for thin slabs (thinner than a wavelength) this mode most closely matches its wave vector with the wave vector of the photon. Below we shall see that for thicker slabs, higher-order modes can have much larger decay rates. We shall also see that the radiative stability of the polariton mode in very thick slabs is a consequence of the fact that the higher-order atomic (excitonic) modes break the longitudinal symmetry of the slab.

II. FRENKEL EXCITON SUPERRADIANT DECAY IN THIN SLABS

In this section we will adopt a model of superradiance originally due to Rehler and Eberly[4] and developed for calculation of superradiant decay of Wannier excitons in single quantum wells by Björk *et al.*[15] In order to conserve space and in order to facilitate for the reader, we will omit the derivation of the model which is well described in Refs. 4, 6, and 15 and we will closely follow the notation in this section with that in Refs. 4, 6, and 15.

The superradiant decay rate in this model, which is based on the exciton pole approximation, can be estimated from three numbers: The number of effective oscillators N, the "shape factor" $\mu \leq 1$ describing the effect of the spatial distribution of the oscillators and the atomic (excitonic) state, and the "fundamental oscillator" lifetime τ_0. The lifetime τ_0 is directly related to the oscillator strength per unit area (or volume) for excitonic emitters with is fixed for a given material. The interesting quantities for our purposes are N and μ.

To compute the radiation pattern it is also convenient to define a wave-vector-dependent cooperativity factor Γ defined by

$$\Gamma(\mathbf{k},\mathbf{k}_1) = |\{\exp[i(\mathbf{k}-\mathbf{k}_1)\cdot\mathbf{r}]\}_{\mathrm{av}}|^2 \ , \tag{1}$$

where the average is to be taken over the positions $\mathbf{r}$ of the atoms, and $\mathbf{k},\mathbf{k}_1$ are the wave vectors of the radiation and the excited atomic system, respectively. In this section we shall assume that $|\mathbf{k}| = n\omega/c_0$, where $\hbar\omega$ is the atomic (excitonic) transition energy, and n is the index of refraction in the slab. From Fig. 1 and from (1) we see that $\exp[i(\mathbf{k}-\mathbf{k}_1)\cdot\mathbf{r}_i]$ is the phase of the field emitted by atom (dipole) i as seen from a far-field reference point O in the $\mathbf{k}$ direction. If the total atomic system is contained in a volume much smaller than a wavelength cubed, $\Gamma(\mathbf{k},\mathbf{k}_1) \equiv 1$, but if the system extends over distances much larger than the wavelength, Γ becomes angularly dependent. In the direction where the radiation wave vector coincides with the atomic-state wave vector (if any such direction exists), so that $\mathbf{k} = \mathbf{k}_1$, Γ is still equal to unity for a large system, but in most directions the emission from the individual excitons will deconstructively interfere to some extent, bringing down the net superradiance of the system.

In this paper we shall mainly be interested in polarized excitations such that $\mathbf{k}_1$ is normal to the slab. Such excitations have no dipole-moment component in the slab normal (z direction), and the unit dipole radiation intensity at time $t = 0$ can be written as

$$I(\varphi,\psi) = \frac{3(\cos^2\varphi + \sin^2\varphi\cos^2\psi)I_0}{8\pi}. \tag{2}$$

The radiation intensity has been normalized so that integrated over all solid angles at time $t = 0$, $\int I(\mathbf{k})d\Omega_{\mathbf{k}} = I_0 = \hbar\omega/\tau_0$. The factor μ is a measure of the net (directionally averaged) cooperativity. It is defined as

$$\mu = \frac{1}{I_0}\int I(\mathbf{k})\Gamma(\mathbf{k},\mathbf{k}_1)d\Omega_k - \frac{1}{N}. \tag{3}$$

For small samples in which all atoms are contained in a volume $\ll \lambda^3$ the factor is always very close to unity since Γ is unity. In larger samples μ is smaller than unity and in one- and two-dimensional sample geometries, μ and N have mutually inverse dependence on the system size.

The decay rate can, to a high accuracy, be approximated by $\mu N/\tau_0$. Below we shall initially compute the decay rate for Frenkel excitons in a crystal slab or molecular films. For simplicity we shall assume that the lattice is cubic with a lattice constant a and with the possibility of harboring one Frenkel exciton in each unit cell. Later we shall generalize the result to a slab of disordered atoms with a well-defined mean density, and to Wannier excitons in a quantum well or a crystal slab. The sample geometry we assume is depicted in Fig. 1.

The crystal slab is assumed to have a thickness h and

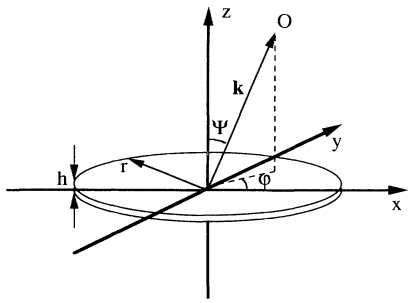

FIG. 1. Schematic drawing of the assumed geometry. The x axis is oriented along the polarization of the slab. The vector $\mathbf{r}_i$ goes from slab matrix site i to the observation point O.

a radius $r \gg \lambda$. At time $t = 0$ the system is assumed to be excited, e.g., by flashing a short pulse of light with constant intensity across the slab. It is important to note that in most experiments r is not given by the physical size of the molecular film, but rather by the radius of the pump pulse. The excitation pulse wave vector is assumed to be normal to the quantum-well plane ($\mathbf{k}_1 \parallel \hat{\mathbf{z}}$). However, we shall let the wave vector of the atomic (excitonic) system be different from that of the emitted radiation ($|\mathbf{k}| \neq |\mathbf{k}_1|$). Creating an excitation with the exciton resonant energy but an arbitrary wave vector can in principle be accomplished by two-photon absorption. In the following we shall neglect the fact that such an excitation can only be set up over lengths (in at least one direction) comparable to the resonant energy wavelength. This is not particularly important in view of the fact that such a mode is only dominant for slab thicknesses comparable to half an emission wavelength anyhow.

The factor N is now trivial to compute. For Frenkel excitons it is given by the number of lattice cells in our system since each cell can host one Frenkel exciton. Hence

$$N = \frac{\pi h r^2}{a^3} = \frac{\pi r^2 M}{a^2} , \tag{4}$$

where M is the number of monoatomic layers in the film. Below we shall come back to the cases of Wannier excitons and randomly ordered atomic systems.

Next, let us compute Γ. For reasons that will become apparent later we shall derive Γ for two specific cases of excitation. One is the excitation of the excitonic mode with a wave-vector length equal to that of radiation at the exciton resonant energy. This mode can easily been excited by a short pulse of light propagating along the slab normal. The other interesting case is that with zero $\mathbf{k}_1$ vector. In the following we will refer to them as case I and case II. The assumptions in the two cases can be stated

$$\mathbf{k}_1 = \begin{cases} 2\pi\hat{\mathbf{e}}_z/\lambda & \text{case I,} \\ \hat{\mathbf{0}} & \text{case II.} \end{cases} \tag{5}$$

In Fig. 2 the excitation of the system is schematically shown. The Frenkel excitons in the slab matrix are depicted as circles. The Frenkel exciton dipole-moment phase is depicted as a clock hand. In (a) the phase rotates by 2π from one side to the other of the wavelength thick slab (case I), whereas in (b) all excitons have the same phase (case II). In (c) the case I excitation is depicted for a thinner slab. In (d) we have depicted a case where $|\mathbf{k}_1| \gg |\mathbf{k}|$. In (e), finally, we have depicted a case where $\mathbf{k}_1$ is not perpendicular to the slab. This case can easily be treated with the formalism in this section, but we will not do it in this paper. Note that to conserve space in the figures, the slab thicknesses (along the z direction) exceed the slab widths in (a) and (b). In our model we always assume the opposite is true.

When computing Γ we need to sum over all the excitons in the film. According to our assumptions, $r \gg h = Ma$ and $\lambda \gg a$ so we can approximate the discrete sum over all the excitons in a monolayer film plane by an integral, assuming that the excitons have a continuous lateral distribution. In both cases I and II, the phase of the excitons is constant throughout the film plane. This integral is effectively the normalized two-dimensional spatial Fourier transform of a circular disk i.e., a Bessel function. Summing over all the film planes we arrive at the expression

$$\Gamma(\mathbf{k}, \mathbf{k}_1) = \begin{cases} \left(\dfrac{2J_1[2\pi r \sin(\psi)/\lambda]}{2\pi r \sin(\psi)/\lambda}\right)^2 \left(\dfrac{\sin\{\pi a M[1-\cos(\psi)]/\lambda\}}{M \sin\{\pi a[1-\cos(\psi)]/\lambda\}}\right]^2 & \text{case I,} \\ \left(\dfrac{2J_1[2\pi r \sin(\psi)/\lambda]}{2\pi r \sin(\psi)/\lambda}\right)^2 \left(\dfrac{\sin[\pi a M \cos(\psi)/\lambda]}{M \sin[\pi a \cos(\psi)/\lambda]}\right)^2 & \text{case II,} \end{cases} \tag{6}$$

where J_1 is the first Bessel function of the first kind, and we have expressed the directional coordinates of $\mathbf{k}$ in the cylindrical coordinates φ and ψ. (Since the system has rotational symmetry, the expressions are independent of the coordinate φ.) It is clear that for a monolayer film, $M = 1$, the expressions (6 I) and (6 II) coincide. However, as the film gets thicker, (6 I) predicts superradiance dominantly in the forward ($\psi = 0$) direction and less in the backward ($\psi = \pi$) direction, whereas (6 II) predicts equal (but smaller) effects in the forward and backward directions. This follows from the symmetry of the assumed initial condition in (5 II). In Fig. 3 emission patterns for the two cases and for various film thicknesses are plotted. Equation (5 I) effectively assumes a coherent transfer of the excitation energy from the excitation pulse to the excitons. Therefore, as the film thickness gets thicker and

the localization of the excitons in this direction is gradually lost, Heisenberg's uncertainty principle suggests that the momentum in the direction normal to the film will be conserved with increasing accuracy. This is the physical basis for the dominant forward emission in this case. The finite lobe width exists even for thick slabs because we have assumed a finite radius slab ($r = 2\lambda$) in the calculation of the patterns. (The lobe full width at half maximum is roughly $\lambda/2r$.) A slab with larger diameter would emit in a narrower lobe, but the essential point in this plot is the gradual increase of unidirectional coupling between the excitons and the radiation modes in case I. The excitons in case II, on the other hand, gradually lose their emission directionality as the film gets thicker. One interpretation of this behavior is that the initial condition of case II does not correspond to a minimum position-momentum uncertainty state. Furthermore, as can be deduced from the magnification scales indicated on the plots, case I represents a superradiant state even for thick slabs, whereas case II represents a superradiant state only for thin (< a wavelength) slabs, and becomes subradiant in thicker slabs. As can be seen from the figure, the radiation rate per exciton for a 5-wavelength-thick slab excited with $|\mathbf{k}_1| = 0$ approaches the rate of a monolayer-thick slab.

In (6) above we actually neglected that the Frenkel exciton state in an ideal slab matrix has a quantized k_1 vector component in the direction normal to the crystal slab or thin film due to the periodicity of the film and the film boundary conditions. In a film M monolayers thick there will be M modes with k_1 vectors $k_1 = 2\pi m/Ma$, where $m = 0 \ldots M-1$ is the mode number. Strictly speaking, the transverse k vector should also be quantized, but due to the large lateral system size one can approximate the closely spaced quantized modes with a continuous distribution of transverse k vectors. Hence (6) above really describes spatially disordered systems (with a mean dipole density of a^{-3}) better than Frenkel excitons in a crystal or molecular film matrix. However, in order for (6) to be valid the disorder fluctuations should be negligible on a spatial scale equal to or larger than a wavelength. Taking the periodic structure of the crystal slab in the normal direction into account, Eq. (6) will be modified as

$$\Gamma(\mathbf{k},\mathbf{k}_1) = \left(\frac{2J_1[2\pi r\sin(\psi)/\lambda]}{2\pi r\sin(\psi)/\lambda}\right)^2 \left(\frac{\sin\{\pi[m - Ma\cos(\psi)/\lambda]\}}{M\sin\{\pi[m/M - a\cos(\psi)/\lambda]\}}\right)^2. \tag{7}$$

Note that for $m = 0$, i.e., $|\mathbf{k}_1| = 0$, Eq. (7) reduces to (6 II). For a q-wavelength-thick slab, where q is an integer, Eq. (7) reduces to (6 I) for the $m = q$ mode. In Fig. 2 the $m = 0$ mode is depicted in (b) and the $m = 1$ mode is depicted in (a) and (d) for two different slab thicknesses.

To calculate the decay rate of the superradiant excitons we have to calculate the parameter μ. Using (3), the unit dipole radiation patterns (2) and (6), and using the transformation $x = \cos(\psi)$, the shape factor is given by

$$\mu = -\frac{1}{N} + \frac{3}{2(2\pi r/\lambda)^2}\int_{-1}^{1}\frac{dx(1+x^2)J_1^2(2\pi r[1-x^2]^{1/2}/\lambda)}{1-x^2}\begin{cases}\left(\dfrac{\sin\{\pi aM[1-x]/\lambda\}}{M\sin\{\pi a[1-x]/\lambda\}}\right)^2 & \text{case I,}\\ \left(\dfrac{\sin(\pi aMx/\lambda)}{M\sin(\pi ax/\lambda)}\right)^2 & \text{case II.}\end{cases} \tag{8}$$

In the limit $r \gg Ma$ this integral is solvable analytically, and the final expression for μ is

$$\mu \approx -\frac{1}{N} + \frac{3}{2(2\pi r/\lambda)^2}\begin{cases}1 + \left(\dfrac{\sin(2\pi aM/\lambda)}{M\sin(2\pi a/\lambda)}\right)^2 & \text{case I,}\\ 2\left(\dfrac{\sin(\pi aM/\lambda)}{M\sin(\pi a/\lambda)}\right)^2 & \text{case II.}\end{cases} \tag{9}$$

If we keep the excitonic modes quantized and calculate μ from Γ given by (7) we arrive at the expression

$$\mu \approx -\frac{1}{N} + \frac{3}{2(2\pi r/\lambda)^2}\left\{\left(\frac{\sin(\pi[m - Ma/\lambda])}{M\sin(\pi[m/M - a/\lambda])}\right)^2 + \left(\frac{\sin(\pi[m + Ma/\lambda])}{M\sin(\pi[m/M + a/\lambda])}\right)^2\right\}. \tag{10}$$

Equations (9) and (10) are the final results that allow us to calculate the decay rate of the excitons in a resonantly excited thin film. The decay rate for a monolayer film can be written as

$$\frac{1}{\tau_1} = \frac{1+\mu N}{\tau_0} = \frac{3}{4\pi\tau_0}\left(\frac{\lambda}{a}\right)^2 \tag{11}$$

for all cases, since in this case only the $m = 0$ mode (with zero wave vector) exists. Hence the superradiant enhancement can be written as $3\pi(c_0/\omega_{ex}an)^2$, where c_0 is the speed of light in vacuum and n is the refractive index of the thin film. This factor is identical to that derived in Refs. 9 and 10 as will be shown below. This factor can be rather large, of the order of 10^5, since the ratio λ/a can be of the order of 10^3. The decay rates for

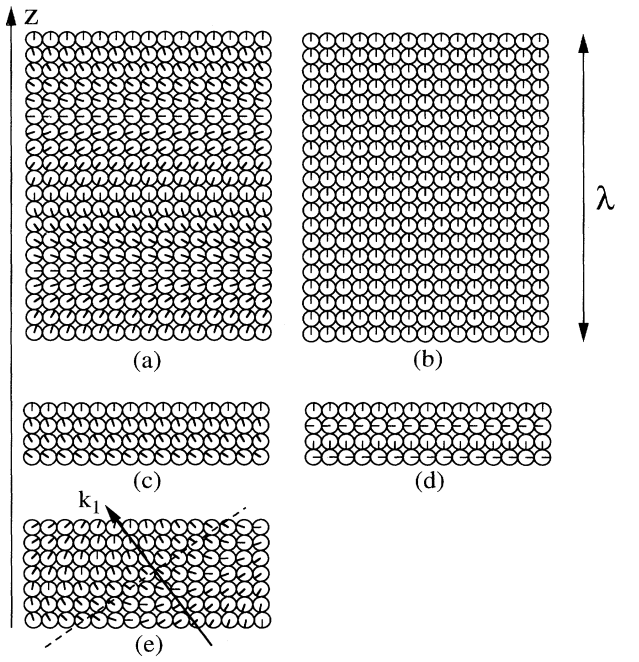

FIG. 2. Schematic drawing of various initial wave-vector states of the excited slab. (a) and (c) represent an initial condition corresponding to case I. (b) corresponds to case II. In (d) $|\mathbf{k}| \ll |\mathbf{k}_1|$ has been assumed, and in (e), the slab wave vector is not perpendicular to the slab. The phases of the excitons along a line perpendicular to $\mathbf{k}_1$ (dashed line) are all equal.

films of arbitrary thicknesses can be expressed,

$$\frac{1}{\tau_{\text{Frenkel}}} = \frac{M}{2\tau_1} \begin{cases} 1 + \left(\dfrac{\sin(2\pi a M/\lambda)}{M \sin(2\pi a/\lambda)} \right)^2 & \text{case I,} \\ 2 \left(\dfrac{\sin(\pi a M/\lambda)}{M \sin(\pi a/\lambda)} \right)^2 & \text{case II.} \end{cases} \tag{12}$$

The extension of this result to (10) is trivial. The result can be rewritten in terms of the oscillator strength per unit volume f and in this case the prefactor changes according to

$$\frac{M}{2\tau_1} = \frac{\pi e^2 a M f}{2 n m_e c_0}, \tag{13}$$

where n is the semiconductor refractive index, e is the unit charge, c_0 is the speed of light in vacuum, and m_e is the electron mass. The two terms in (12 I) have a physical interpretation, the first term is the radiation emitted in the forward ($\mathbf{k} = \mathbf{k}_1$) direction, whereas the second term is the radiation emitted in the backward direction. In (12 II), these terms are equal due to the initial state symmetry; hence the factor 2 to the right of the curly bracket. It is seen that in case II the radiation in the backward direction increases with thickness for thin slabs, but becomes smaller again when the slab thickness is larger than about half a wavelength. This is dictated by momentum conservation.

In Fig. 4 we have plotted the superradiant decay rate normalized to the monolayer superradiant rate $1/\tau_1$ as a function of the number of layers for the two cases. For case I, it can be seen that the decay rate is proportional to M for large M:s. The decay rate is predicted to increase without bounds as the film gets thicker. For case II ($m = 0$), Knoester[9,10] pointed out that there is an optimum decay rate of $0.23\lambda/a\tau_1$ when $h = 0.37\lambda$. For large M, (12 II) predicts that, the decay rate approaches zero as $1/M$. It is clear from these results that, depending on the initial conditions of the collective wave function, the same model predicts completely different results. This was pointed out by Dicke in his original paper. One may create both superradiant and subradiant states in a col-

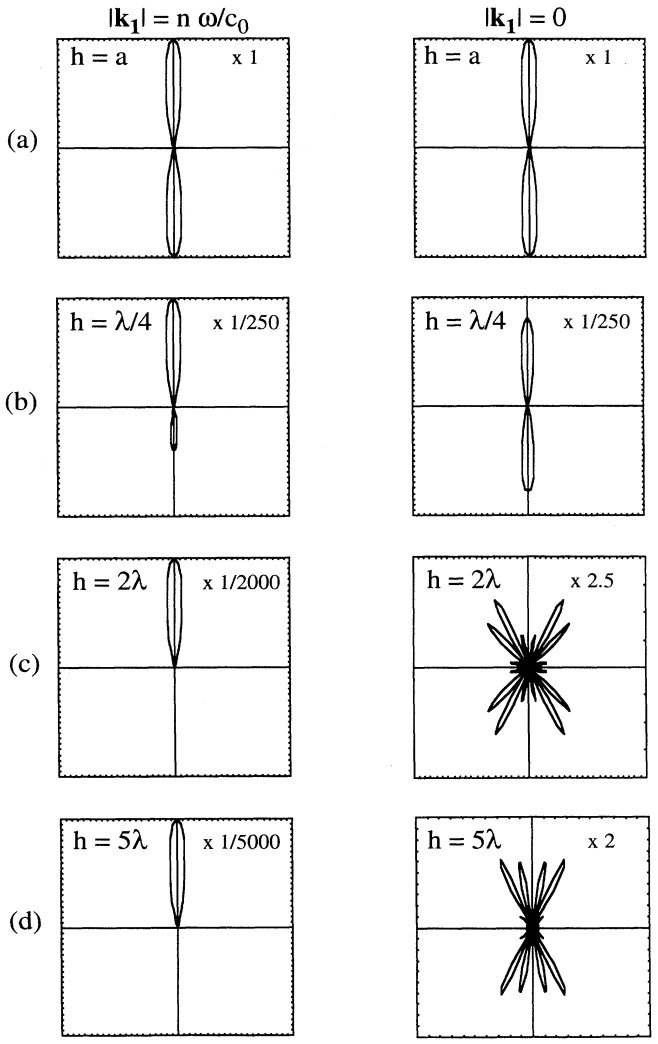

FIG. 3. Radiation patterns for various slab thicknesses. The plotted entity is the radiated intensity per exciton. In the left column are the patterns for case I ($k = \omega/c$), and in the right column are the patterns for case II ($k = 0$). The number to the right in each figure is the plot scaling factor. Hence, the 5-wavelength-thick case I slab emits 5000 times more radiation in the forward direction than the monolayer slab.

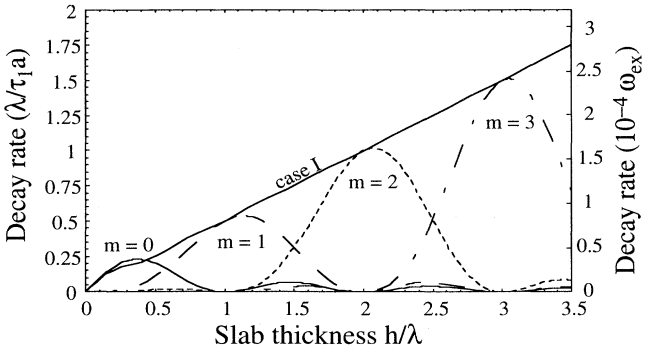

FIG. 4. The normalized decay rate of a slab with superradiant Frenkel excitons as a function of the normalized film thickness h/λ. In this and following graphs we have assumed $\lambda/a = 10^3$ and $\Delta/\omega_{ex} = 0.01$. The solid diagonal line corresponds to case I, whereas the solid quasiperiodic curve is case II ($m = 0$). The quantized solutions for $m = 1, \ldots, 3$ are drawn as dashed and dash-dotted curves. It is seen that the case I curve is the envelope function of the decay rates for the quantized modes. The decay predicted by (12 I) is never more than a factor of 2 from the correct value.

lection of emitting particles. However, neither (12 I) nor (12 II) is correct in the limit $M \to \infty$. This was first pointed out by Arecchi and Courtens,[7] who argued that since retardation effects are not correctly taken into the model, it is incorrect to extrapolate the results to large, spatially extended systems. In Sec. IV below, we shall see that Arecchi and Courtens' objections to the indiscriminate use of (12 I) above arise as a consequence of making the exciton pole approximation in the derivations above. In Fig. 4 we have also plotted the results for the quantized modes. It is seen that with quantized modes the decay rate will essentially be increasing as a function of slab thickness, but with a modulation due to the discretization of the excitonic modes. In a "classical" optics picture, this "modulation" of the decay rate (or equivalently, for the time reversed process, absorption) can be described as a Fabry-Pérot effect due to the susceptibility mismatch at the slab boundaries. It is seen that for a slab x wavelengths thick, the maximally radiant state is the mode with an m which minimizes $|m - x|$. This is due to k-vector conservation.

III. EXTENSION TO ATOMS AND WANNIER EXCITONS

The results above easily extend to atomic systems and Wannier exciton systems as well. Hence, superradiance in the weak excitation regime has little to do with the internal structure of the constituent state dipoles and is mainly determined by the collective state wave function.

The extension to atomic systems is straightforward. In this case the unit dipole radiator is the isolated atom which has a well-defined lifetime. In a disordered system, the atomic dipole moments will be randomly distributed. However, only the in-plane dipole in a fixed direction can contribute to the superradiance. Therefore, although on the macroscopic scale the atomic system is spatially isotropic, the radiation pattern of an excited dipole will still be anisotropic due to the anisotropic initial condition and will be given by (2). If the geometric shape of the atomic system is still slab shaped, (12 I) is also still valid with aM replaced by the slab thickness h and τ_1 replaced by the appropriate constant factor. In this case only case I is strictly valid since neither the transverse nor the longitudinal $\mathbf{k}$ vectors are quantized. Therefore, strictly speaking, it is not correct to talk about a $|\mathbf{k}_1| = 0$ mode. The number of atoms is given by $N = \rho\pi r^2 h$, where ρ is the mean atomic density per unit volume in the slab. Inserting these replacements in the expressions for τ_1 one gets

$$\frac{1}{\tau_{\text{Atom}}} = \frac{3\rho\lambda^2 h}{8\pi\tau_0}\left[1 + \left(\frac{\sin(2\pi h/\lambda)}{2\pi h/\lambda}\right)^2\right]. \tag{14}$$

The equation assumes that the atomic density $\rho \gg \lambda^{-3}$ since the derivation assumes a continuous distribution of dipoles on the wavelength scale. Also, as mentioned above, it assumes negligible density fluctuations on wavelength (and longer) scales. In the equation λ is the wavelength of light in the atomic medium. We see that (14) predicts a linear dependence of the superradiant decay rate with atomic density and an essentially linear dependence on the slab thickness h. Both these predictions are due to the pole approximation.

Next, consider a moderately thick slab of material which supports Wannier excitons. In this case it is convenient to express the decay rate in the material oscillator strength and it is quite natural to identify the number of unit dipoles with

$$N = \frac{\pi r^2 h}{4\pi a_B^3/3} = \frac{3r^2 h}{4a_b^3}, \tag{15}$$

which is the slab volume divided by the exciton Bohr volume (a_B is the exciton Bohr radius). Furthermore, the decay constant τ_0 and the oscillator strength f per unit volume can be tied by the unit radiator dipole matrix element Ξ. The expressions are

$$\frac{1}{\tau_0} = \frac{4ne^2\omega_{ex}^3|\Xi|^2}{3\hbar c_0^3}, \tag{16}$$

and

$$f = \frac{2m\omega_{ex}|\Xi|^2}{\pi\hbar a_B^3}. \tag{17}$$

Hence, combining (9 I), (11), (15), (16), and (17) we get

$$\frac{1}{\tau_{\text{Wannier}}} = \frac{3\pi e^2 hf}{4nmc_0}\left[1 + \left(\frac{\sin(2\pi h/\lambda)}{2\pi h/\lambda}\right)^2\right]. \tag{18}$$

The equation assumes that the slab is at least a few Bohr radii thick. If not, the Wannier wave function will become deformed by the longitudinal confinement.[21] In this latter case, when the slab thickness (or quantum well, in

other words) is on the order of a Bohr radius the superradiant decay rate becomes

$$\frac{1}{\tau_{QW}} = \frac{2\pi e^2 f_{2D}}{nmc_0}, \tag{19}$$

where f_{2D} is the oscillator strength per unit area, as derived in Refs. 15 and 22. In principle it should be possible to interpolate between the two equations (18) and (19), but in reality it may be simpler to employ a formalism such as that developed in Refs. 21 and 23 that derives the self-energy from first principles, taking the deformation of the wave function explicitly into account.

To summarize this section we have shown that within the pole approximation, the model derived by Rehler and Eberly can treat atomic and excitonic superradiance of thin and thick slabs in a unified manner.

IV. THE POLE APPROXIMATION-FREE EQUATION OF MOTION

Knoester[9,10] derived a more correct description of the dipole field interaction in a thin crystal slab or molecular film. Specifically both the static dipole-dipole interaction and the radiation-exciton interaction are properly included in the theory without resorting to pole approximations. Knoester showed that the coupled exciton-radiation field dispersion relation can be written

$$\omega^2 - \omega_{ex}^2 - 2\omega F_{kk} = 0, \tag{20}$$

where

$$F_{kk}(M,\omega) = \frac{a\Delta^2}{8Mc}\left\{\frac{\sin(M\Phi^-)}{\sin^2(\Phi^-)}\exp(-iM\Phi^-) - \frac{\sin(M\Phi^+)}{\sin^2(\Phi^+)}\exp(iM\Phi^+)\right\} + \frac{\omega\Delta^2}{2c^2}\sum_{j=-\infty}^{\infty}\{(w/c)^2 - (k+2\pi i/a)^2\}^{-1}, \tag{21}$$

and

$$\Phi^{\pm} \equiv a(k_1 \pm \omega/c)/2. \tag{22}$$

The constant Δ in (21) is a measure of the oscillator strength. Below we shall express Δ in oscillator strength and in the decay rate of a single localized Frenkel exciton.

As pointed out by Knoester, Eqs. (20)–(22) above are easy to solve in two different limits, namely, for very thin and very thick slabs. In the former case, one considers F_{kk} to be a small perturbation in the exciton dispersion relation. In this case, one arrives at the excitonlike mode eigenfrequency

$$\omega \approx \omega_{ex} + F_{kk}(M,\omega_{ex}). \tag{23}$$

This is the exciton pole approximation. We shall see below that in general it has both a real and an imaginary part. In the second limit, when $M \to \infty$, the first term of (21) containing the sine functions tends to zero for long lengths, and furthermore one can approximate the sum in (21) by the $j = 0$ term only. It is found that by doing so, the dispersion relation (20) becomes an eigenfrequency equation,

$$\omega^2 - \omega_{ex}^2 - \frac{\omega\Delta^2}{\omega^2 - \omega_{ex}^2} = 0, \tag{24}$$

with the approximate mode eigensolutions (angular frequencies)

$$\omega \approx \omega_{ex} \pm \Delta/2. \tag{25}$$

We note that the solutions are radiatively stable (i.e., real) and represent the two (odd and even) polariton modes in the system. We are now in a position to identify Δ as the difference in the polariton (angular) frequency. The entity $\hbar\Delta$, expressed in energy or wavelength, is often referred to as the exciton-polariton vacuum Rabi splitting.

In order to derive expressions for the decay rates under the exciton pole approximation, we begin by noting that F_{kk} has singularities when $k + 2\pi j/a = \omega/c$. Otherwise it is a well-behaved function. Neglecting the umklapp process contributions to the sum in (21), only the $i = 0$ term remains. The remaining singularity can be removed, however, by defining $F_{kk}(M,kc)$ as

$$F_{kk}(M,kc) \equiv \lim_{w\to kc} F_{kk}(M,\omega). \tag{26}$$

One hence obtains

$$F_{kk}(M,kc) = \frac{\Delta^2}{8\omega_{ex}}\left\{1 - \frac{\sin(2\pi aM/\lambda)\cos(2\pi aM/\lambda)}{2\pi aM/\lambda} - i\frac{aM\omega_{ex}}{c}\left[1 + \left(\frac{\sin(2\pi aM/\lambda)}{2\pi a/\lambda}\right)^2\right]\right\}. \tag{27}$$

From this equation, using the definition of Δ^2,

$$\Delta^2 = \frac{8\pi\omega_{ex}e^2|\Xi|^2}{\hbar n^2 a^3}, \tag{28}$$

and Eq. (16) we exactly recover the result (12 I). [Note that the imaginary part of (27) is the amplitude decay rate, whereas the rate (12 I) is the excitation (energy) decay rate.] Furthermore, by combining (28) above with

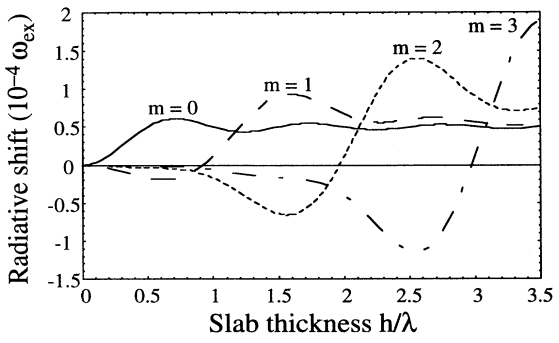

FIG. 5. The normalized radiative shifts ($\omega - \omega_{ex}$ in units of $10^{-4}\omega_{ex}$) of a slab with superradiant Frenkel excitons as a function of the normalized film thickness h/λ. The radiative shifts of the four lowest modes are shown.

(17) we can express the polariton mode difference energy in an infinitely thick slab in the oscillator strength per unit volume f as $\hbar\Delta = \hbar(2\pi e^2 f/n^2 m)^{1/2}$.

Equation (27) confirms that at least at the crossing point, Knoester's formalism, combined with the pole approximation, is identical to the usual atomic superradiance model (12). In fact, if the energy decay rates ($-2\Im\{F_{kk}\}$) for the the various modes, where $\Im$ stands for the imaginary part, are plotted as a function of slab thickness, Fig. 4 is exactly reproduced. However, in addition to the modified decay rate predicted in Secs. II and III, Knoester's model also predicts a radiative shift ($\Re\{F_{kk}\}$). In Fig. 5, the radiative shifts (in units of $10^{-4}\omega_{ex}$) are plotted. Such shifts should of course be expected from general principles; their magnitudes have also been estimated by previous calculations.[11,23] Unfortunately, the shifts for slabs of wavelength thicknesses are so small that they are difficult to detect experimentally.

We must keep in mind that (27) is an approximation. In Fig. 6 the dispersion curves for the relevant modes for 10-, 40-, and 100-wavelength-thick slabs are plotted. It is seen that within the exciton pole approximation, the dispersion for all three slabs looks like a regular dispersion curve, but with increasing decay rates and frequency shifts. The general solutions to (20) and (21) are difficult to get analytically, but are relatively straightforward to obtain numerically. The exact solution of the excitonlike solution of (20) for a 10-wavelength-thick slab is equal to that plotted in Fig. 6(a) to within the resolution of the plot. The exact dispersion of the excitonlike mode of the 40-wavelength-thick slab differs very slightly from that derived within the exciton pole approximation, and it differs only for the three modes closest to $m = h/\lambda$. The cross and the two open circles in Fig. 6(b) show the correct dispersion points for those modes; for all the other modes the points in the figure coincide with the exact dispersion. For the 100-wavelength-thick slab the exact dispersion is quite different from that plotted in Fig. 6(c). The exact dispersion for both modes for the three listed cases is plotted in Fig. 7. One of the dispersion branches has been interconnected by line segments to guide the eye. It is seen that for the 100-wavelength-thick slab, the modes cross over, and the photonlike branch for $m < 100$ becomes an excitonlike branch when $m > 100$. The dispersion curves look remarkably similar to those derived for microcavity-embedded quantum-well excitonic radiation derived in Ref. 13.

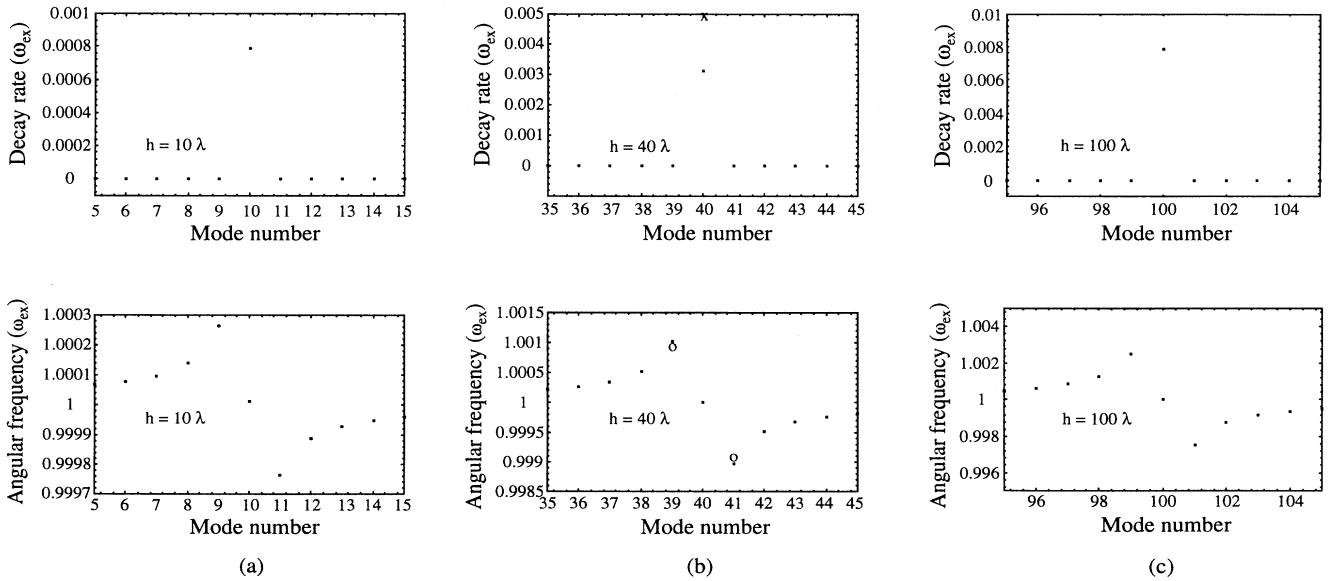

FIG. 6. The normalized dispersion (in units of ω_{ex}), derived from the exciton pole approximation, of the excitonlike mode for three slab thicknesses. The open circles for modes 39 and 41 and the cross for mode 40 in (b) are the correct points if the dispersion is solved without resorting to the exciton pole approximation.

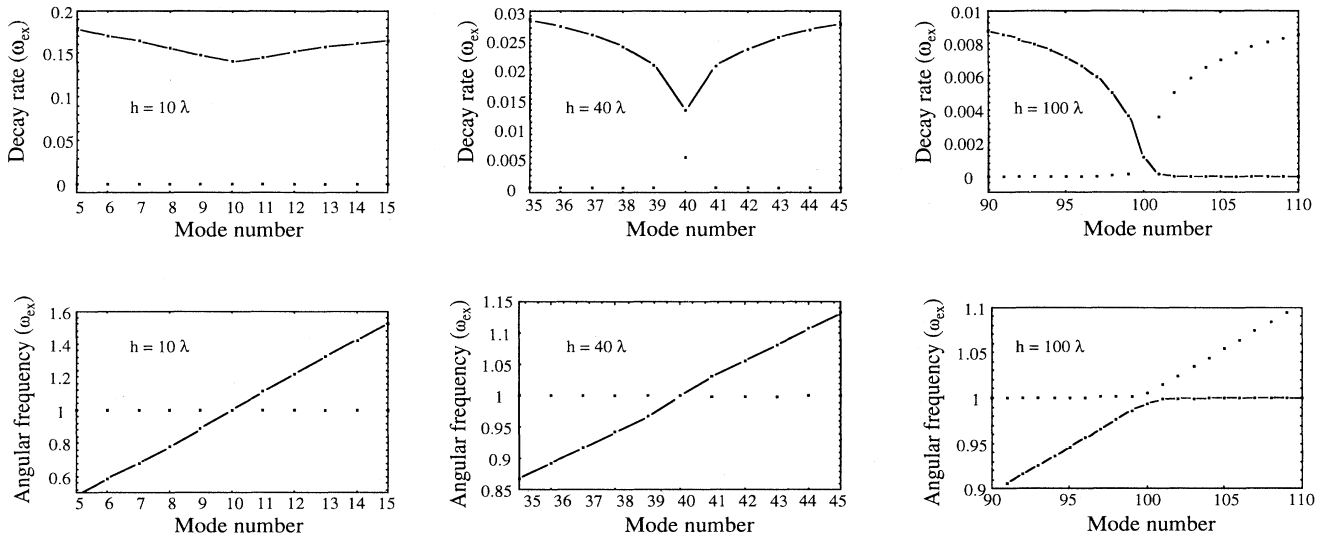

FIG. 7. The normalized dispersion (in units of ω_{ex}), derived from the dispersion relation, for three slab thicknesses. The dispersion of both system modes is displayed. In (a) and (b) the interconnected series of points represents the photonlike mode. In (c) the interconnected mode crosses over from a photonlike to an excitonlike mode.

V. THE SUPERRADIANCE TO POLARITON CROSSOVER AND THE POLARITON POLE APPROXIMATION

In Sec. III we derived results showing that the atom superradiance and Wannier- and Frenkel-exciton superradiance are all manifestations of essentially the same physics in the low excitation regime. The main difference is that the periodic structure in molecular or crystalline slabs quantizes the $\mathbf{k}_1$ vector, whereas in a slab where the atom location is sufficiently random it is justified to use m as a continuous (real) number.

It is also clear from (12) and (27) that in the exciton pole approximation, the decay rate of the $m = h/\lambda$ mode increases without bounds. In this section we show that the exact solution of (20) actually shows a saturation of the decay at a fixed slab thickness.

In Fig. 8 we have drawn the eigenfrequencies of the two coupled radiation-exciton modes at the $kc = \omega_{ex}$ point. We have deliberately only plotted the values for slab thicknesses equal to a multiple of wavelengths, so that the $m = h/\lambda$ mode exactly fulfills the condition. From arguments presented above, the maximum deviation from this curve is a factor of 2 in decay rate for slabs with thicknesses an odd multiple of half wavelengths thick. We see that for thin slabs, as expected, the photonlike mode has a much larger decay rate than the excitonlike mode. However, at and above the crossover point (at about 44 wavelengths in the present example), the modes have identical decay rates but instead the real part of the eigenfrequencies becomes different. This is the true exciton-polariton crossover behavior. The result looks remarkably similar to the exciton-superradiance to exciton-polariton crossover in a single quantum-well microcavity.[16] A difference between the slab calculation and the microcavity calculation is the frequency shift of the photonlike mode for thin slabs. Note that these small shifts (on the order of a few percent of the exciton eigenfrequency) cannot be seen in Fig. 7.

While it is difficult to derive an exact analytical expression for the crossover point, it is relatively straightforward to derive an approximate expression. The crossover roughly takes place when $-\Im\{F_{kk}(M, kc)\} = \Delta$. Hence, the maximum superradiant decay rate is approximately Δ. From (27) it can be seen that the decay rate for thick slabs approximately is given by $\Delta^2 h/4c$, where $h = Ma$ is the physical thickness of the slab. The crossover length is therefore approximately given by

$$h_{\text{cross}} = \frac{4c}{\Delta} = 2c_0\sqrt{\frac{m}{\pi e^2 f}} \approx \frac{cT_{\text{Rabi}}}{2} = \frac{\omega_{ex}\lambda}{2\Delta}, \qquad (29)$$

where $T_{\text{Rabi}} = 2\pi/\Delta$ is the Rabi flopping cycle time and c is the velocity of light in the medium. For the parameters used in Fig. 8, the corresponding length is 50 wavelengths, and we see that the crossover takes place in a slab 44 wavelengths thick. We also see that the fastest "superradiant" decay is about 1.6Δ, slightly faster than the predicted maximum decay rate of Δ.

In Fig. 8 we also have plotted the decay rate (12 I) predicted in the exciton pole approximation. It is seen that at the crossover point, the exciton pole approximation gives a slightly smaller decay rate of 0.7Δ. However, it is also seen that for slab thicknesses smaller than about $cT_{\text{Rabi}}/4$, the decay rate predicted by the exciton pole approximation is excellent. The radiative shift predicted by the exciton pole approximation is always smaller than or equal to $\Delta^2/8\omega_{ex}$. This is effectively zero to within the

resolution of Fig. 8 (b).

In Ref. 9 Knoester introduced the polariton pole approximation to give a simplified and divergence-free expression for the polariton mode (amplitude) decay (above the crossing point) as

$$\gamma_{k1}(M) = -\frac{\omega_{k1}^2 - (kc)^2}{\omega_{k1}^2 - \omega_{k2}^2} \Im\{F_{kk}(M, \omega_{k1})\}, \qquad (30)$$

where the indices $k1$ and $k2$ refer to the two polariton branches and γ_{k1} and ω_{k1} are the decay rate and the angular frequency of polariton branch 1. Permutation of the two indices gives the decay rate for the second branch.

True polariton modes exist only when the exciton and the photon wave vectors match, i.e., when $kc = \omega_{ex}$. When the wave vectors match, the polariton modes have identical effective masses and damping rates. This is the situation we are primarily interested in. We can also use the fact that the polariton mode eigenfrequencies are approximately given by $\omega_{k1} \approx \omega_{ex} - \Delta/2$ and $\omega_{k2} \approx \omega_{ex} + \Delta/2$. When we insert these relations into (30) and note that the sum in $F_{kk}(M, \omega)$ is real and therefore does not contribute to (30), we can derive the approximate expression for the polariton mode (amplitude) decay as

$$\gamma_{k1}(M) \approx \frac{c}{aM} \sin^2(Ma\Delta/4c). \qquad (31)$$

As noted by Knoester this is an oscillating function with the slab thickness. The maximum (energy) decay predicted by this model is very close to $\Delta/\pi \approx 0.3\Delta$, which occurs for a slab thickness Ma slightly smaller than $\omega_{ex}\lambda/\Delta$. Again the approximate values for the decay rate and the crossover length are quite close to the exact results . The oscillatory behavior of the polariton decay in the polariton pole approximation is a mathematical artifact and does not correspond to the actual physics. In reality, the envelope function of $\gamma_{k1}(M)$ describes the decay rate for the system in a better way. Knoester argued that for slab thicknesses larger than the crossover thickness, the $\sin^2$ function in (31) should be replaced by its effective (or rather mean) value 1/2. By doing so the (energy) decay rate of the polariton modes become

$$2\gamma_{k1}(M) \approx \frac{c}{aM} = \frac{c}{h}. \qquad (32)$$

This result has an obvious physical interpretation. The polariton modes decay with a rate given by the time it takes for the modes to propagate across the crystal. [Note, however, that the polariton mode group velocity is not c but $c/2$ (Ref. 24).] This is consistent with the macroscopic view that the radiative energy decay from an ideal crystal must take place through the crystal's surrounding interfaces. In Fig. 8 the (energy) decay rates $2\gamma_{k1}(M)$ predicted by the polariton pole approximation (30) and by its envelope function $2c/h$ are plotted dash-dotted and dotted, respectively. We see that for slab lengths around 100λ the two curves predict equal decay rates, roughly a factor of 2 above the rate calculated by the exact dispersion relation. For a slab thickness of 200λ (and 400λ, 600λ, ...), (31) predicts a decay rate several orders of magnitude smaller than the actual decay rate. Equation (32), on the other hand, gives a decay rate very close to the exact value.

To give some numerical results, we have used parameters appropriate for a molecular film in our plots where the ratios λ/a and Δ/ω_{ex} have been chosen to be 10^3 and 0.01, respectively. In this case it is seen that the maximum decay rate is about 51 000 times the monolayer excitonic superradiant rate, and about 220 times faster than the maximum decay rate of the $m = 0$ mode. Hence, the behavior $m = 0$ mode as a function of slab thickness has nothing to do with the superradiance to polariton mode crossover. The subradiance of the $m = 0$ mode in thicker slabs is not due to the formation of a polariton, but is a consequence of the mode symmetry.

In GaAs, which has $\hbar\omega_{ex} = 1.515$ eV and a polariton mode splitting Δ of about 20 meV, one gets a maxi-

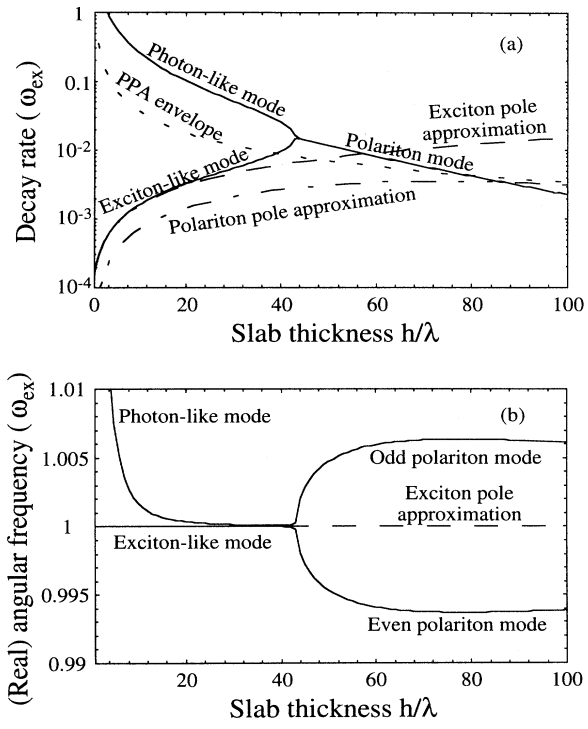

FIG. 8. The decay rate and radiative shifts of the two system modes with $m = h/\lambda$ as a function of the normalized slab thickness h/λ. The system changes from a superradiant to a polaritonic system at a slab length of 44λ. The dashed line represents the predicted decay rate for the excitonlike mode using the exciton pole approximation. The dash-dotted line represents the predicted decay rate of the polariton modes using the polariton pole approximation while the dotted line represents the polariton pole approximation (PPA) envelope function. The agreement between (one half) this envelope function and the exact polariton solution is excellent for slab thicknesses greater than about twice the crossover thickness (about 100λ for the parameters above).

mum superradiant decay rate of 20 fs. The Rabi period time T_{Rabi} is about 100 fs. The slab length corresponding to the superradiance to polariton crossover behavior is about 9 μm. In thicker slabs this is also the polariton beat oscillation length (polariton-pulse propagation length during one Rabi cycle), since the group velocity of the polariton mode at $k = \omega_{ex}/c$ is half that of light propagation.[24] Hence, in order to observe polariton propagation effects in bulk GaAs, the sample should be a few tens of microns thick. It should be possible to map out the excitonlike modes' and the polariton modes' eigenfrequencies for different slab thicknesses using a tunable narrow linewidth cw laser looking at the absorption spectrum. The experiment must be carried out at cryogenic temperatures since the Rabi frequency is only an order of magnitude or so larger than the dephasing rate due to phonon scattering, even at 4 K. The photonlike mode is going to be virtually impossible to detect due to its very rapid decay. It should also be possible to measure the decay rates and the polariton mode beating (Rabi oscillation) in the time domain using a tunable femtosecond laser as the excitation source. It is probably going to be difficult to resolve the modes close to the crossover point since the time scales of the photonlike mode and excitonlike mode are equal. Therefore the pump pulse (propagating like a photonlike mode) will mask excitonlike mode response. However, for slabs thin (but not too thin) and thick compared to the crossover thickness it still should be possible to observe all but the photonlike branch. Finally, it should be pointed out that in most materials, GaAs included, the excitonic (atomic) dispersion has several branches. The analysis in this paper is simplistic in that respect since all but one exciton (atom) dispersion branch is neglected.

VI. CONCLUSIONS

In this paper we have compared a conventional atomic superradiance model with the more rigorous dispersion model of arbitrary thickness molecular films or semiconductor slabs. It was demonstrated that the two models are equivalent within the exciton pole approximation of the latter. It was also shown that over a wide range of slab thicknesses the exciton pole approximation is excellent.

If the rigorous dispersion model is solved, the behavior of thin slabs, superradiance, is transformed into polariton propagation when the slab becomes sufficiently thick. We computed an approximate expression for the maximum superradiant decay rate and for the slab thickness at which this maximum superradiance occurs. Our expression is close, but slightly better than that predicted by the polariton pole approximation. We showed that, as expected, the excitonic mode with the closest **k**-vector match to that of the light will always couple most strongly to radiation modes (both in the superradiant and in the polariton regimes). Modes with poorly matched k vectors can be subradiant. Finally, we remarked that the superradiance to polariton crossovers in slabs and in microcavity-embedded thin slabs are remarkably similar, in spite of the difference between the dispersion relations of the free-photon modes and the cavity-photon modes.

ACKNOWLEDGMENTS

The authors would like to thank Professor J. Knoester of the University of Groningen, the Netherlands and Dr. L. C. Andreani of the Università di Pavia, Italy for stimulating discussions. S.P. gratefully acknowledges financial support from the John and Fannie Hertz Foundation.

[1] R. H. Dicke, Phys. Rev. **93**, 99 (1954).
[2] V. Ernst and P. Stehle, Phys. Rev. **176**, 1456 (1968).
[3] D. P. Craig and L. A. Dissado, Proc. R. Soc. London Ser. A **325**, 1 (1971).
[4] N. E. Rehler and J. H. Eberly, Phys. Rev. A **3**, 1735 (1971).
[5] Y. C. Lee and P. S. Lee, Phys. Rev. B **10**, 344 (1974).
[6] L. Allen and J. H. Eberly, *Optical Resonance and Two-level Atoms* (John Wiley & Sons, New York, 1975).
[7] F. T. Arecchi and E. Courtens, Phys. Rev. A **2**, 1730 (1970).
[8] E. Hanamura, Phys. Rev. B **38**, 1228 (1988).
[9] J. Knoester, Phys. Rev. Lett. **68**, 654 (1992).
[10] J. Knoester, J. Lumin. **53**, 101 (1992).
[11] Y.-C. Lee, D.-S. Chuu, and W.-N. Mei, Phys. Rev. Lett. **69**, 1081 (1992).
[12] J. J. Hopfield, Phys. Rev. **112**, 1555 (1958).
[13] K. Odani, Y. Ohfuti, and K. Cho, Solid State Commun. **87**, 507 (1993).
[14] D. S. Citrin, IEEE J. Quantum Electron. **30**, 997 (1994).
[15] G. Björk, S. Pau, J. Jacobson, and Y. Yamamoto, Phys. Rev. B **50**, 17 336 (1994).
[16] V. Savona, L. C. Andreani, P. Schwendimann, and A. Quattropani, Solid State Commun. **93**, 733 (1995).
[17] S. Pau, G. Björk, J. Jacobson, H. Cao, and Y. Yamamoto, Phys. Rev. B **51**, 14 437 (1995).
[18] G. S. Agarwal, J. Opt. Soc. Am. B **2**, 480 (1985).
[19] T. Tokihiro, Y. Manabe, and E. Hanamura, Phys. Rev. B **51**, 7655 (1995).
[20] J. Jacobson, S. Pau, H. Cao, G. Björk, and Y. Yamamoto (unpublished).
[21] L. C. Andreani, A. d'Andrea, and R. del Sole, Phys. Lett. A **168**, 451 (1992).
[22] L. C. Andreani, F. Tassone, and F. Bassani, Solid State Commun. **77**, 641 (1991).
[23] D. S. Citrin, Phys. Rev. B **47**, 3832 (1993).
[24] S. Pau, G. Björk, J. Jacobson, H. Cao, and Y. Yamamoto, Phys. Rev. B **51**, 7090 (1995).